Charges dispersed over the permeation pathway determine the charge selectivity and conductance of a Cx32 chimeric hemichannel

Seunghoon Oh, Vytas K. Verselis and Thaddeus A. Bargiello

Department of Neuroscience, Albert Einstein College of Medicine, Bronx, NY 10461, USA

Previous studies have shown that charge substitutions in the amino terminus of a chimeric connexin, Cx32*43E1, which forms unapposed hemichannels in *Xenopus* oocytes, can result in a threefold difference in unitary conductance and alter the direction and amount of open channel current rectification. Here, we determine the charge selectivity of Cx32*43E1 unapposed hemichannels containing negative and/or positive charge substitutions at the 2nd, 5th and 8th positions in the N-terminus. Unlike Cx32 intercellular channels, which are weakly anion selective, the Cx32*43E1 unapposed hemichannel is moderately cation selective. Cation selectivity is maximal when the extracellular surface of the channel is exposed to low ionic strength solutions implicating a region of negative charge in the first extracellular loop of Cx43 (Cx43E1) in influencing charge selectivity analogous to that reported. Negative charge substitutions at the 2nd, 5th and 8th positions in the intracellular N-terminus substantially increase the unitary conductance and cation selectivity of the chimeric hemichannel. Positive charge substitutions at the 5th position decrease unitary conductance and produce a non-selective channel while the presence of a positive charge at the 5th position and negative charge at the 2nd results in a channel with conductance similar to the parental channel but with greater preference for cations. We demonstrate that a cysteine substitution of the 8th residue in the N-terminus can be modified by a methanthiosulphonate reagent (MTSEA-biotin-X) indicating that this residue lines the aqueous pore at the intracellular entrance of the channel. The results indicate that charge selectivity of the Cx32*43E1 hemichannel can be determined by the combined actions of charges dispersed over the permeation pathway rather than by a defined region that acts as a charge selectivity filter.

(Received 7 January 2008; accepted after revision 21 March 2008; first published online 27 March 2008)
Corresponding author T. A. Bargiello: Department of Neuroscience, Kennedy Center, Albert Einstein College of Medicine, 1410 Pelham Parkway South, Bronx, NY 10461, USA. Email: bargiell@aecom.yu.edu

Historically, vertebrate gap junction channels have been described as large non-selective pores that allow the passage of molecules up to ∼1 kDa. This view was based largely on early studies that reported the permeability of gap junctions found in cardiac and liver tissues to large fluorescent anionic dyes such as Lucifer Yellow and 6-carboxyflourescein (minimal molecular diameter ∼9.5 and ∼8.5 Å, respectively). Studies of exogenously expressed connexins have shown that connexin channels display a large diversity in their pore diameter, single channel conductance, permeability and charge selectivity and there appears to be no simple relation between the permeability of connexin channels to large molecules, their unitary conductance and their charge selectivity (Harris, 2001, 2007). However, due to the large pore diameter of connexin channels, it is reasonable to expect that differences observed in permeation and selectivity of connexin channels will involve factors such as the limiting pore diameter, surface charge, and the distribution of fixed charges along the permeation pathway.

An estimate of pore size with neutral molecules has been accomplished for relatively few connexin channels. The radius of human Cx32 intercellular channels has been estimated to be between 6 and 7 Å (Oh *et al.* 1997), while the pores of Cx26, Cx37, Cx43 and Cx40 appear to be somewhat smaller (see Harris, 2001). Of these, Cx40 intercellular channels appear to be the smallest as they are not permeable to mannitol and stachyose (radius 6.4 Å, Beblo & Veenstra, 1997). The unitary conductance of intercellular channels ranges from ∼10 pS for Cx30.2 (Bukauskas *et al.* 2006) to ∼340 pS for Cx37 (Banach *et al.* 2000) in recording solutions containing 100–150 mM KCl. Notably, the unitary conductance of Cx26 intercellular channels (∼150 pS) is substantially greater

 DOI: 10.1113/jphysiol.2008.150805

than that of Cx32 (∼70 pS) despite its smaller pore size, indicating that factors other than pore diameter can determine unitary conductance. Similarly, despite its low unitary conductance, Cx30.2 intercellular channels allow the passage of dyes up to 400 Da (Rackauskas *et al.* 2007).

Brink (1983) and Verselis & Brink (1986) have demonstrated that both small ions and larger dye molecules permeate earthworm gap junctions as hydrated species. For the most part, the conductance of small metal ions for a given connexin channel is predicted by their mobility in bulk solution (Oh *et al.* 1997) as expected for a large diameter pore although small deviations have been reported (Wang & Veenstra, 1997; Beblo & Veenstra, 1997). There is little or no discrimination between similarly charged metal cations. Connexin channels do, however, vary considerably in their charge selectivity. Cx46 intercellular channels and unapposed hemichannels are substantially cation selective: P_K/P_{Cl} ∼13 when the extracellular surfaces is exposed to low ionic strength solutions (Trexler *et al.* 2000), whereas Cx32 intercellular channels are slightly anion selective in a gradient of 100 mM to 10 mM CsCl (P_K/P_{Cl} ∼0.6; Oh *et al.* 1997). Bukauskas *et al.* (2002) reported that the open state of the intercellular Cx43 channel is non-selective, whereas substates induced by V_j-gating are anion selective, suggesting that the conformational changes accompanying V_j-gating alter the structure of the permeation pathway. Qu & Dahl (2002) have reported that closure of the voltage gate of Cx43 and Cx46 preferentially restricts the passage of fluorescent tracer molecules and cAMP and proposed that the physiological role of the voltage gate is to selectively restrict the passage of large molecules between cells while allowing electrical coupling.

The cation selectivity of Cx46 hemichannels is determined primarily by charged residues located in the first extracellular loop, E1 (Trexler *et al.* 2000; Kronengold *et al.* 2003). Unitary conductance and open channel rectification of Cx46 hemichannels can also be influenced by residues contained in the first transmembrane segment (M1) and the N-terminus (NT) (Ma & Dahl, 2006; Hu *et al.* 2006; Srinivas *et al.* 2006). These results support the view that M1, E1 and NT contribute to the formation of the channel pore. Dong *et al.* (2006) report that the N-terminus plays a critical role in determining molecular permeability and voltage gating of Cx45.6 gap junctional channels and Banach *et al.* (2000) have suggested that cytoplasmic surface charge influence the conductance of human Cx37 gap junction channels.

In studies of the molecular determinants of V_j-gating, Purnick *et al.* (2000*a*) and Oh *et al.* (2004) reported that negative charge substitutions in the N-terminus substantially increased the unitary conductance of unapposed Cx32*43E1 hemichannels and linearized the current–voltage relations of the open state. Positive charge substitutions at the same positions decreased unitary conductance and slightly increased the inward rectification of the parental Cx32*43E1 channel. These results suggested that charges in the N-terminus are pore lining and may be important determinants of ion permeation through the Cx32*43E1 hemichannel. Here, we determine the charge selectivity of the Cx32*43E1 channel and channels containing negative charges at either the 2nd, 5th or 8th positions, a positive charge at the 5th position, and a double mutation containing a positive charge at the 5th position and negative charge at the 2nd position. We demonstrate that T8C residue is modified by a methanethiosulphonate reagent further supporting the view that the N-terminus forms the cytoplasmic entrance of the channel. Our findings indicate that while charged residues in the extracellular segments appear to play a substantial role in establishing the charge selectivity of Cx32*43E1 channels, the structure of the hemichannel permits charge substitutions in the N-terminus to also have a large role in determining charge selectivity. These results imply that there is no defined region, common to all connexin channels, that determines charge selectivity.

Methods

Construction of chimeric connexins, site-directed mutagenesis, RNA synthesis and oocyte injection

The procedures have been described by Oh *et al.* (1999). Cx32*43E1 is a chimera in which the first extracellular loop of Cx32 (E1) amino acids 41–75 has been replaced with that of Cx43 amino acids 42–76. Cx43 and other Group 2 connexins (with the exception of Cx45) contain an additional amino acid at the 2nd position (see Bennett *et al.* 1994). Cx32 is classified as a Group 1 connexin. A sequence alignment of the E1 domains of Cx32, 43 and 46 is presented in Table 1. Mutations carrying charge substitutions at the 2nd, 5th and 8th positions were constructed by standard procedures using synthetic oligonucleotides and the polymerase chain reaction.

Electrophysiological recordings and analysis

Single channel data were acquired using pCLAMP 7.0 software, an Axopatch 200B integrating patch amplifier, and a Digidata 1200A interface (Axon Instruments, Inc.). Current–voltage relations were obtained from excised patches with ∼1.3 s, ±70 mV voltage ramps. Data were acquired at 5 kHz and filtered at 1 kHz with a four pole Bessel filter.

Experiments were performed in a RC11 recording chamber (Warner Instruments, Hamden, CT, USA). The bath solution volume was between 500 and 750 μl. In all experiments, the pipette solution contained (mM): 100 KCl, 2 EGTA, 2 EDTA, 10 Hepes, adjusted to pH 7.6

Table 1. Aligned sequence of the first extracellular loop of Cx32, 43 and 46

	41	51	61	71
rat Cx32	**E**SVWG**DE*K***SSFICNTLQPGCNSVCY**D**HFFPISHV***R***			
rat Cx43	**E**SAWG**DE**QSAF***R***CNTQQPGC**E**NVCY**D*K***SFPISHV***R***			
rat Cx46	**EE**VWG**DE**QS**D**FTCNTQQPGC**E**NVCY**D*R***AFPISHI***R***			

Negatively charged amino acids are in bold, positively charged amino acids are italicized. Amino acid residues are numbered with respect to Cx32. The first residue in E1 of Cx32 is the 42nd residue in Cx43 and Cx46.

Table 2. Summary of measured reversal potentials and P_K/P_{Cl} ratios of wild-type and mutant channels

Bath solution (mM KCl)		500 mM		200 mM		50 mM		20 mM		10 mM	
KCl activity		325		144		41		17		9	
Channel		I/O	O/O	I/O	O/O	I/O	O/O	I/O	O/O	I/O	O/O
43E1	E_{rev} ± S.D.	−8.3 ± 2.2	11.7 ± 3.1	−3.6 ± 0.8	4.0 ± 2.1	2.4 ± 1.8	−6.0 ± 2.1	7.9 ± 3.6	−21.1 ± 4.3	8.9 ± 5.7	−30.6 ± 3.3
	No. of patches	3	3	4	8	15	4	13	6	3	4
	P_K/P_{Cl}	1.7	2.1	1.6	1.7	1.4	2.2	1.6	4.1	1.6	5.2
N2E	E_{rev} ± S.D.	−23.8 ± 1.7	32.3 ± 2.4	−11.8 ± 1.4	12.6 ± 1.6	6.4 ± 2.6	−5.9 ± 2.1	22.3 ± 4.9	−16.2 ± 3.7	33.5 ± 5.7	−33.3 ± 5.0
	No. of patches	3	6	17	10	10	3	9	6	5	3
	P_K/P_{Cl}	5.7	19.7	6.8	8.7	2.4	2.2	4.6	2.8	6.3	6.2
N2E*	E_{rev}*	−22.3		−11.6		12.0		31.7		42.2	
	P_K/P_{Cl}*	4.8		6.5		7.1		13.3		12.8	
G5D	E_{rev} ± S.D.	−31.6 ± 2.4	28.5 ± 4.9	−16.9 ± 0.9	15.4 ± 1.4	6.8 ± 1.1	−7.8 ± 1.7	19.7 ± 2.1	−18.9 ± 3.8	32.4 ± 2.9	−35.3 ± 2.8
	No. of patches	4	5	4	9	8	7	8	7	6	6
	P_K/P_{Cl}	16.9	10	> 50	> 50	2.5	3.0	3.7	3.5	5.8	7.1
T8D	E_{rev} ± S.D.	−15.6 ± 3.1	27.1 ± 1.1	−8.8 ± 2.0	10.7 ± 2.1	7.3 ± 2.9	− 4.2 ± 1.5	14.2 ± 4.2	− 12.1 ± 2.6	28.6 ± 4.6	−27.3 ± 1.5
	No. of patches	10	5	12	9	15	6	17	7	6	4
	P_K/P_{Cl}	2.8	8.3	3.5	5.2	2.7	1.7	2.5	2.1	4.6	4.2
G5R	E_{rev} ± S.D.	−0.6 ± 5.1	3.7 ± 3.5	−0.6 ± 2.3	−1.9 ± 2.4	0.9 ± 1.2	2.3 ± 3.2	−0.9 ± 4.3	−3.5 ± 4.7	3.2 ± 6.4	−7.2 ± 3.0
	No. of patches	3	2	14	5	4	4	6	6	3	2
	P_K/P_{Cl}	1.0	1.3	1.1	0.8	1.1	0.7	1.0	1.2	1.2	1.4
N2E + G5R	E_{rev} ± S.D.	−17.0 ± 1.5	14.4 ± 0.1	−8.2 ± 1.8	7.0 ± 2.4	6.3 ± 1.3	−5.3 ± 1.1	13.6 ± 2.5	−17.6 ± 1.7	26.3 ± 3.7	−31.7
	No. of patches	5	2	17	7	7	11	7	4	7	1
	P_K/P_{Cl}	3.2	2.6	3.2	2.6	2.3	2.0	2.4	3.1	4.0	5.6

I/O, inside-out, O/O, outside-out. Reversal potentials and P_K/P_{Cl} ratio for a long lived N2E inside-out patch.

with 1 M KOH. Patches were excised into a bath solution of the same composition and instrumentation offsets were corrected manually. The bath chamber was connected by a 3 M KCl agar bridge to a ground chamber containing the same solution as the recording pipette. The initial bath solution was exchanged by gravity perfusion of ∼5 ml of solutions containing (mM): 10, 20, 50, 200, or 500 KCl, 2 EGTA, 2 EDTA, 10 mM Hepes, pH 7.6. The excised patch was repeatedly perfused with different bath solutions until either the channel disappeared or the seal was lost. In most cases reversal potentials for a given patch could be obtained for only a subset of different KCl solutions.

Reversal potentials (E_{rev}) were determined by fitting an exponential or linear function of voltage to the open state current recorded during voltage ramps. The E_{rev} for a given solution was the average of those obtained in three to five consecutive voltage ramps. The reversal potentials reported in Table 2 are the mean and standard deviation (S.D.) of multiple patches. The ratio of cation to anion permeability was determined from reversal potentials using the Goldman–Hodgkin–Katz (GHK) equation (see Eisenman & Horn, 1983).

Estimates of leak current could not be obtained, as complete channel closures by the 'loop gating' mechanism were rarely observed with the application of ±70 mV ramps. In most cases, experiments were terminated because of the loss of seal integrity and thus leak conductance could not be estimated from the residual current following channel loss. In channels with active V_j-gating (e.g. N2E), only patches containing at most two channels were analysed to avoid variation attributable to possible differences in the selectivity of substates and the open state. In cases where little or no gating was observed over the voltage range employed (e.g. Cx32*43E1) reversal potentials calculated from patches containing multiple channels were included. In most cases Cx32*43E1 patches contained one or two channels as assessed by the current level recorded at −70 mV in symmetric 100 mM KCl solutions.

Results

Cx32*43E1

Cx32*43E1 is a chimera in which the first extracellular loop of Cx32 (residues E41–R75) is replaced with that of Cx43 (residues E42–R76). A sequence alignment of the E1 domain of Cx32, Cx43 and Cx46 is presented in Table 1. The amino acid sequence of the E1 domain of Cx32 and Cx43 differs in nine positions and includes a difference in charge at four positions, Cx32K48Q, Cx32I52R, Cx32N61E and Cx32H67K. Although the position of charged residues differs, the net charge of Cx32, −2, is not changed by the substitution of the Cx43 E1 segment. In contrast, the net charge of E1 is −5 in Cx46.

To examine the charge selectivity of open Cx32*43E1 hemichannels, reversal potentials were measured in excised patches in which the external surface of the patch was exposed to a series of salt gradients ranging from 10 to 500 mM KCl. In all cases, the internal solution contained 100 mM KCl. Traces illustrating the current–voltage relations and changes in reversal potentials for Cx32*43E1 channels are presented in Fig. 1. The average reversal potentials and corresponding P_K/P_{Cl} ratios, calculated with the Goldman–Hodgkin–Katz (GHK) equation, are summarized in Table 2. To facilitate comparisons, the absolute values of the reversal potentials are plotted as a function of the bath salt concentration in Fig. 2*A*.

The cation selectivity of Cx32*43E1 hemichannels is largest in outside-out patches when the extracellular surface of the channel, formed by the two extracellular loops, E1 and E2, is bathed in low ionic strength KCl (10 mM). The measured reversal potential (E_{rev}) of −30.6 ± 3.3 mV corresponds to a P_K/P_{Cl} of ∼5.2 using the ionic activities presented in Table 2. The cation selectivity is reduced as the salt concentration of the external bath solution is increased (Table 2, Fig. 2*A*). In inside-out patches, in which the extracellular surface of the channel is always exposed to 100 mM KCl, the measured reversal potentials of the Cx32*43E1 hemichannel are smaller relative to those obtained in outside-out patches at all salt concentrations (Fig. 2*A*) and do not change substantially when the intracellular surface of the channel is exposed to different concentrations of KCl. (Fig. 2*A*). The difference in the reversal potentials of outside-out and inside-out is greatest at low salt concentrations and is less when either the intracellular surface (inside-out patches) or the

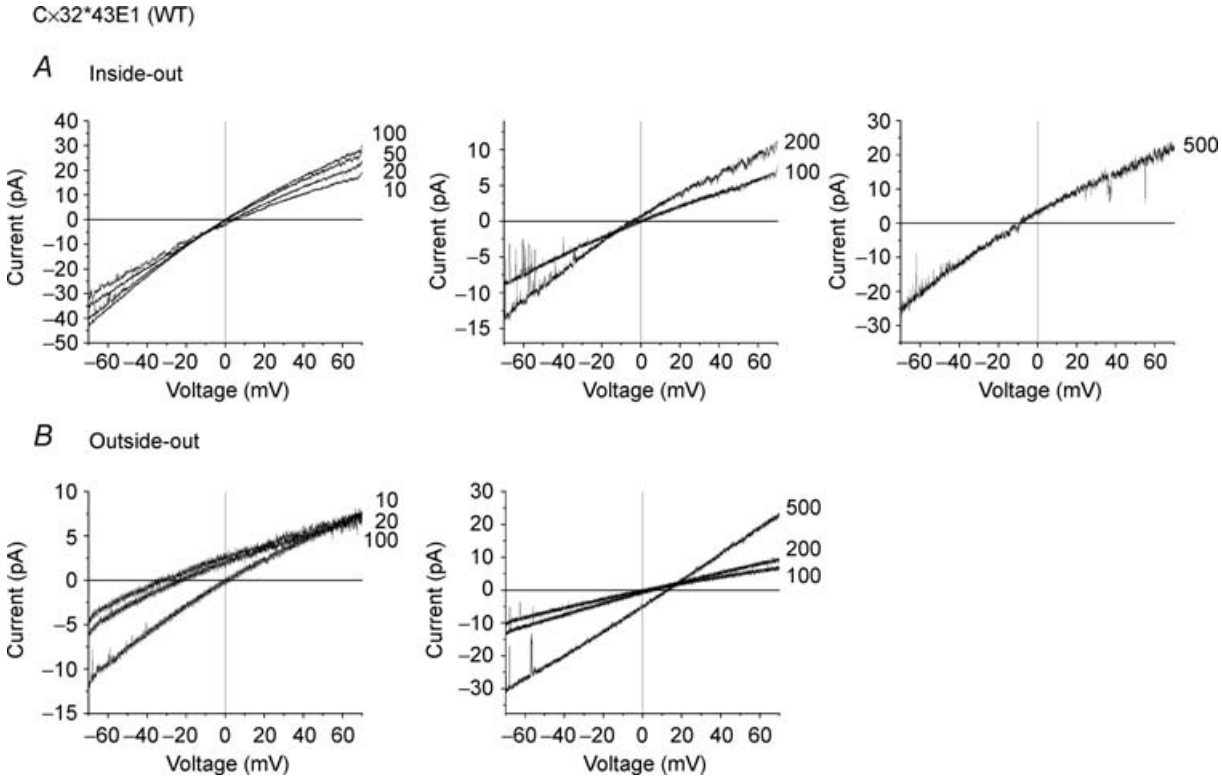

Figure 1. Current–voltage relations of Cx32*43E1 (43E1) channels
A, selected traces illustrating the change in reversal potentials of the open state of 43E1 channels obtained with inside-out patches. The concentration of the KCl in the bath solution is provided next to the current trace. *B*, reversal potentials obtained with outside-out patches. In all cases, the pipette solution contained 100 mM KCl. Current traces were obtained with the application of ±70 mV voltage ramps and digitally filtered at 500 Hz for presentation.

extracellular surface (outside-out patches) is exposed to high salt.

Charge substitutions in the N-terminus

We have proposed that the first 10 amino acid residues of Cx32 form the entry of the channel pore (Purnick *et al.* 2000*a*,*b*). Negative charge substitutions at the 2nd, 5th and 8th position of Cx32*43E1 hemichannels reverse the V_j-gating polarity, linearize the open channel *I–V* relation in symmetric recording solutions, and increase the single channel conductance (Oh *et al.* 2004). The single channel conductances of N2E and G5D in symmetric 100 mM KCl solutions are more than twice that of the parental Cx43E1 channel, 260 ± 31 pS, 240 ± 46 pS and 113 ± 21 pS, respectively, while that of T8D is intermediate, 160 ± 30 pS (Table 3).

N2E. Traces illustrating the open channel current–voltage relations as a function of salt concentration for Cx32N2E*43E1 in inside-out and outside-out patches are presented in Fig. 3. The average reversal potentials and P_K/P_{Cl} ratios of N2E hemichannels are presented in Table 2. Included in Table 2 are the reversal potentials obtained for a long-lived inside-out patch of a single N2E hemichannel (italicized numbers). The long life of the channel in this patch allowed the collection of a complete data set (10 mM to 500 mM KCl) with at least three perfusions at each salt concentration and consequently provides the best comparison of the relative effect of varying the salt concentration on the exposed intracellular surface of this channel.

The absolute values of the reversal potentials for inside-out and outside-out patches of the N2E channels are plotted in Fig. 2*B*. The absolute value of the reversal potential obtained with 500 mM external–100 mM internal KCl is greater than the reversal potential obtained with the reverse gradient, 500 mM internal–100 mM external (32.3 ± 2.4 mV *versus* 23.8 ± 1.7 mV). The average reversal potentials obtained with low salt concentrations in the bath are similar for inside-out and outside-out patches in the averaged data set. The reversal potentials obtained with the long-lived patch are greater than those obtained on average in low salt conditions. As illustrated in Table 2, the reversal potential measured with 10 mM KCl is 42.2 mV, which corresponds to a P_K/P_{Cl} ratio of 12.8. We suspect that the reversal potentials obtained for inside-out patches in low salt conditions may be underestimated in experiments where repeated perfusions could not be obtained. Possible sources of error include incomplete solution exchanges and the presence of an 'unstirred' layer that could arise as a consequence of the geometry of the membrane in inside-out patches (see Gil *et al.* 1999). Only averaged data are used in comparisons of the charge selectivity of mutant hemichannels.

The major feature of the N2E data set is the marked increase in the reversal potential and hence the cation selectivity of the N2E hemichannel in inside-out patches relative to the parental Cx32*43E1 hemichannel at all salt concentrations. This is illustrated in Fig. 2*C*. In outside-out patches, the reversal potentials of N2E and 43E1 hemichannels are comparable in low salt conditions but differ substantially in high salt (Fig. 2*D*). This result indicates that the cation selectivity of the N2E hemichannel is greater than that of Cx32*43E1 when the extracellular surface of either hemichannel is exposed to high salt, but that the cation selectivity is similar when the extracellular surface of these hemichannels is bathed in low salt.

G5D. The effects of the G5D substitution on the charge selectivity of the Cx32*43E1 hemichannel are fundamentally equivalent to those of N2E (Table 2). The principal difference between N2E and G5D hemichannels is the similarity in the absolute value of the reversal potentials for G5D in inside-out and outside-out patches in all salt conditions (Table 2 and Fig. 2*E* and *F*). In contrast the absolute value of the reversal potential of N2E in 500 mM salt is less in inside-out patches. The reversal potential obtained for outside-out G5D patches with 200 mM KCl, 15.4 ± 1.4 mV, is likely to be overestimated as it gives an unreasonably high value for the cation selectivity of the G5D hemichannel in 200 mM KCl. The P_K/P_{Cl} ratio calculated with the GHK equation exceeds 50 for this condition and reflects the extreme sensitivity of the logarithmic function to small changes in reversal potential.

The single channel conductance of the G5D, slightly less than that of N2E (Table 3), and the current–voltage relation in symmetric 100 mM KCl is linear for G5D (not shown, see Oh *et al.* 2004) compared to slight outward rectification of N2E in symmetric salt.

T8D. The addition of a negative charge at the 8th amino acid position in the N-terminus (T8D) increases the unitary conductance of the Cx32*43E1 hemichannel but much less than negative charge substitution at either the 2nd or the 5th position (Table 3). The conductance of T8D hemichannel, 160 pS in 100 mM KCl, is midway between that of the Cx32*Cx43E1 hemichannel (115 pS) and that of the average of N2E and G5D hemichannels (~250 pS). The change in unitary conductance correlates with the reduced charge selectivity of T8D as judged by the comparison of reversal potentials (Fig. 2*C* and *D*). The differences in the reversal potentials of T8D, N2E and 43E1 are more pronounced in inside-out recordings, which expose the intracellular surface of the hemichannel to variable ionic strength solutions. In these cases, T8D

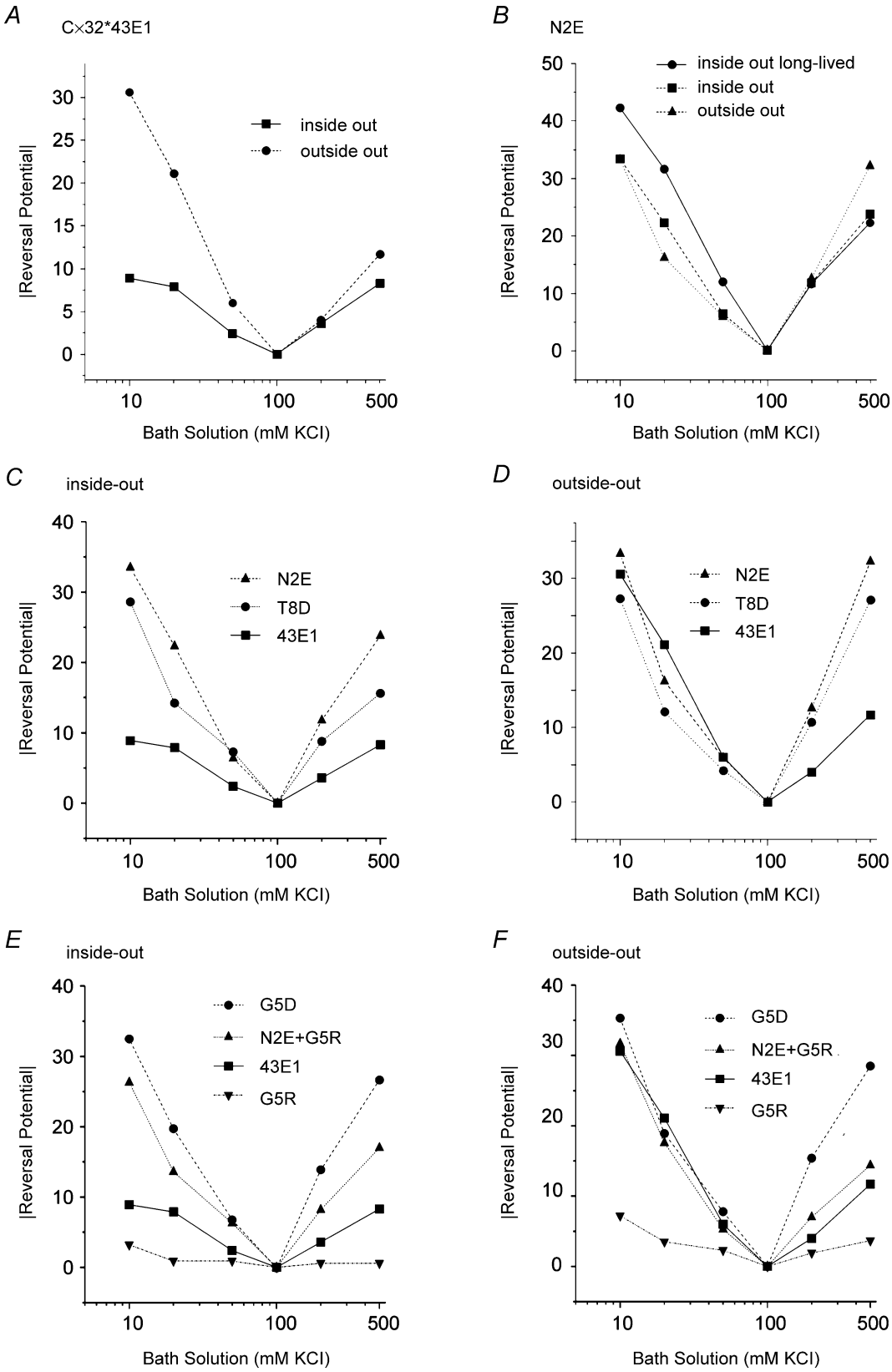

Figure 2. Plot of the absolute value of reversal potentials as a function of ionic strength
A, the absolute values of the average reversal potentials of Cx32*43E1 channels presented in Table 1 for inside-out and outside-out patches are plotted against the bath solution concentration of KCl. *B*, the absolute values of

Table 3. Summary of single channel conductance in symmetric 100 mm KCl

Channel	43E1	N2E	G5D	T8D	G5R	N2E + G5R
Slope conductance (pS) ± S.D.	113 ± 21	260 ± 31	240 ± 46	160 ± 30	79 ± 16	119 ± 25
No. of patches	24	30	11	32	22	26

always displays intermediate values of reversal potentials (Fig. 2*C*). In outside-out recordings, differences in reversal potentials among N2E, T8D and 43E1 hemichannels are only seen with bath salt concentrations of 200 and 500 mM (Fig. 2*D*).

G5R. Current traces illustrating the current–voltage relations of G5R open hemichannels in excised patches exposed to a variety of salt conditions are presented in Fig. 4. The addition of a positive charge at the 5th residue reduces the unitary conductance of the parental Cx32*43E1 hemichannel from 113 ± 21 pS to 79 ± 16 pS measured as the slope conductance at 0 mV in symmetric 100 mM KCl and maintains inward current rectification through the open state in the symmetric salt condition. The conductance is threefold less than that of the G5D channel (240 ± 46 pS). Similar reductions in unitary conductance are observed in channels formed by other positive charge substitutions in the N-terminus including N2R or K (70 pS), G5K (70 pS) and T8R or K (80 pS), Oh *et al.* (2004). The reduction in unitary conductance is accompanied by a large reduction in cation selectivity. The G5R hemichannel is non-selective in the ionic conditions tested, i.e. the reversal potentials are all close to 0 mV in both inside-out and outside-out patch configurations in all ionic conditions (see Table 2 and Fig. 2*D* and *E*).

N2E + G5R. The unitary conductance of the hemichannel formed by the double mutation containing a negative charge at the 2nd position and a positive charge at the 5th position is similar to Cx32*43E1 (119 ± 25 pS and 113 ± 21 pS, respectively). A similar effect is observed for other double mutations at these positions. The unitary conductance of N2E + G5K channel is ∼120 pS (slope conductance at 0 mV in 100 mM KCl) while that of N2R + G5D is ∼105 pS in 100 mM KCl (Oh *et al.* 2004).

The reversal potentials of the N2E + G5R hemichannels obtained with excised patches are compared with those of G5D, G5R and Cx32*43E1 in Fig. 2*E* and *F*. In outside-out patches the reversal potentials of N2E + G5R are virtually identical to those of the parental Cx32*43E1 unapposed hemichannel (Fig. 2*F*) and the direction of current rectification is similar in all bath solutions, rectifying outwardly in 500 mM salt and inwardly in all other salt conditions examined (not shown). However, in inside-out patches, the reversal potentials of the double mutations are intermediate to those of G5D (N2E) and Cx32*43E1 and similar to T8D (Fig. 2*E*). This suggests that the negative charge at the 2nd position has a larger effect in determining the charge selectivity of the channel than does the positive charge at the 5th position. If the two opposite charges neutralized each other, then the charge selectivity would be expected to be similar to that of Cx32*43E1 in both inside-out and outside-out patches. Interestingly, the direction of rectification in the *I–V* relations of N2E + G5R, N2E + G5K and N2R + G5D appears to correlate with the sign of the charge predicted to be closest to the cytoplasmic entrance. In cell-attached patches, the *I–V* relation of N2R + G5D is linear like that of G5D, while those of N2E + G5R and N2E + G5K display inward rectification although less than G5R (see Oh *et al.* 2004).

Taken together, the data suggest that while there is some degree of neutralization among opposite charges located at the 2nd and 5th positions, charges at the 2nd position appear to have a larger effect in determining the charge selectivity of the channel, while the sign of the more external charge at the 5th position appears to play a larger role in shaping the current–voltage relation of the open channel.

reversal potentials of N2E channels for inside-out and outside-out patches are plotted against the bath solution concentration of KCl. Data from Table 1 are plotted for the mean values of outside-out and inside-out patches as well as those obtained from a long-lived inside-out patch. *C*, the absolute values of the average reversal potentials presented in Table 1 for inside-out patches of wild-type (Cx32*43E1, abbreviated 43E1), N2E and T8D are plotted against the bath solution concentration of KCl. *D*, the absolute values of the average reversal potentials presented in Table 1 for outside-out patches of wild-type (Cx32*43E1, abbreviated 43E1), N2E and T8D are plotted against the bath solution concentration of KCl. *E*, the absolute values of the average reversal potentials presented in Table 1 for inside-out patches of Cx32*43E1 (abbreviated 43E1), G5D, G5R and N2E + G5R channels are plotted against the bath solution concentration of KCl. *F*, the absolute values of the average reversal potentials presented in Table 1 for outside-out patches of Cx32*43E1 (abbreviated 43E1), G5D, G5R and N2E + G5R channels are plotted against the bath solution concentration of KCl. Bath solutions concentrations are plotted logarithmically to facilitate comparisons at low and high salt concentrations.

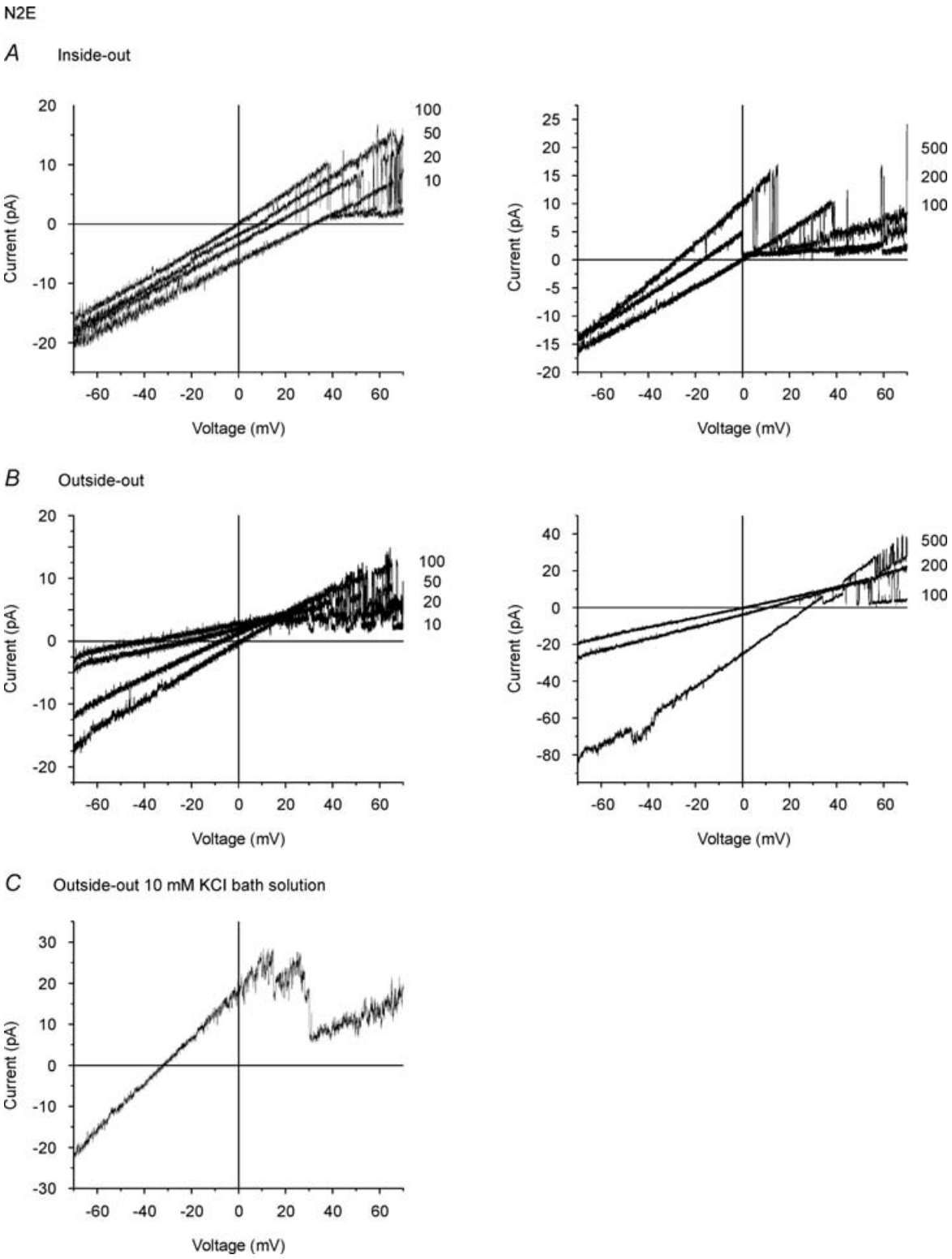

Figure 3. Current–voltage relations of N2E channels
A, selected current–voltage traces illustrating the change in reversal potentials of the open state of a single N2E channel obtained with inside-out patches. The concentration of the KCl in the bath solution is provided next to the current trace. *B*, current–voltage relation of N2E channels obtained with outside-out patches. The concentration of the KCl in the bath solution is provided next to the current trace. *C*, the current–voltage relation of an outside-out patch containing several N2E channels in 10 mM KCl bath solution. In all cases, the pipette solution contained 100 mM KCl. Current traces were obtained with the application of ±70 mV voltage ramps and digitally filtered at 500 Hz for presentation.

Modification of the T8C substitution by MTSEA biotin-X

Our previous studies of the determinants of V_j-gating polarity and the structure of N-terminal peptides indicate that the first 10 amino acids of the N-terminus of Cx32 and Cx32*Cx43E1 form the cytoplasmic entrance of the channel pore. These studies predict that residues N2, G5 and T8 are likely to line the aqueous channel pore. To investigate this possibility further we examined if a cysteine substitution at the 8th position, T8C, was accessible to modification by the thiol modification reagent 2-((6-((biotinoyl)amino)hexanoyl)amino)ethylmethanethiosulfonate (MTSEA biotin-X, Biotium, Hayward, CA). Figure 5 illustrates nine stepwise changes in conductance of two open channels recorded in an inside-out configuration following the application of 1 mM MTSEA biotin-X. The simplest interpretation of the data is that 5 of 6 T8C residues are accessible to modification by this reagent when a single channel resides in the open state. The result supports the view that the T8 residue lines the channel pore and based on the NMR derived structure of the N-terminus (Purnick *et al.* 2000*a*) suggests that residues N2 and G5 would also line the pore. Cysteine substitutions at the second position (N2C) do not express current as homomeric unapposed hemichannels.

Discussion

Cx32*43E1 forms hemichannels that have a preference for cations. Cation selectivity increases substantially when

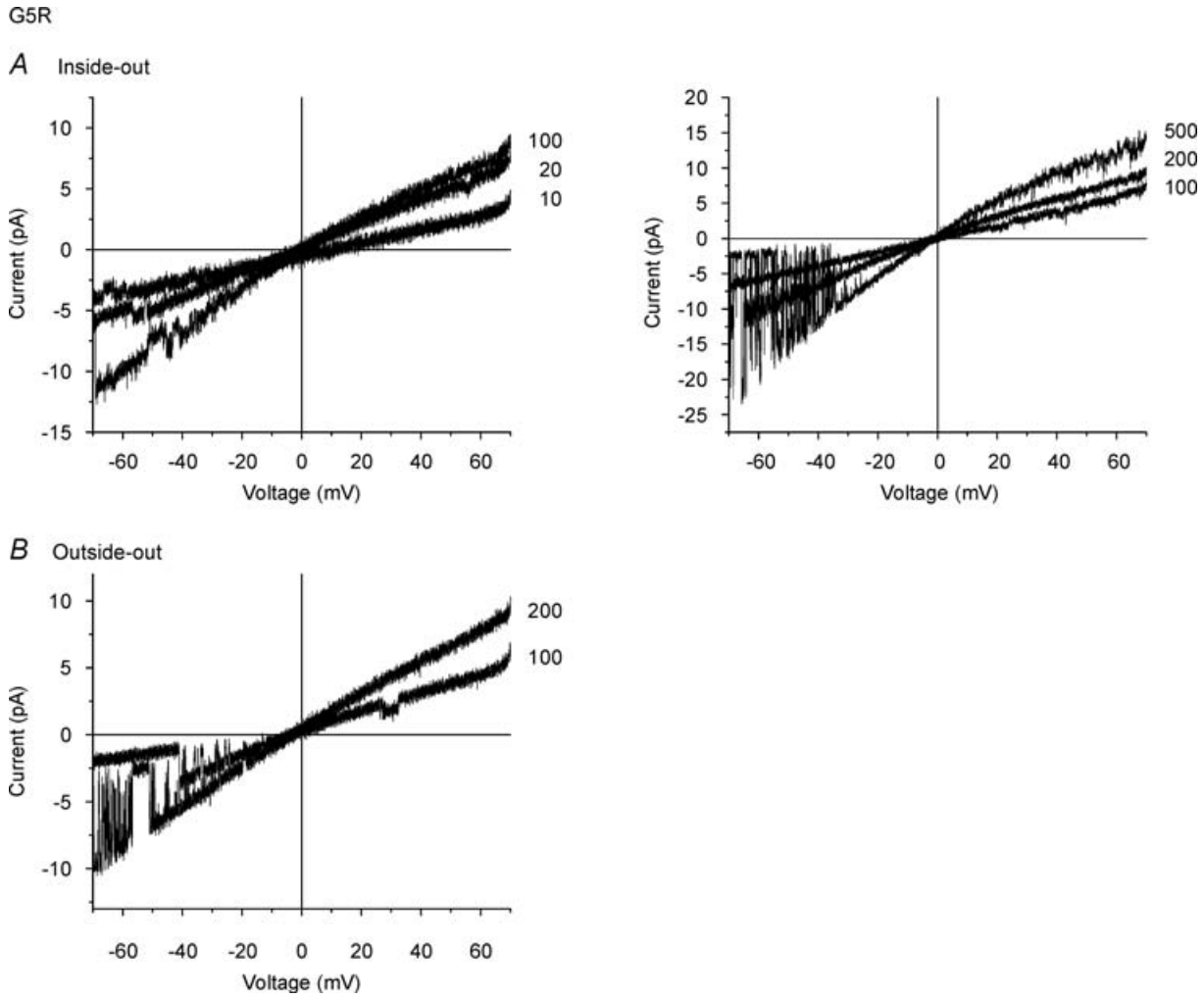

Figure 4. Current–voltage relations of G5R channels
A, selected current–voltage traces illustrating the change in reversal potentials of the G5R channels obtained with inside-out patches. The concentration of the KCl in the bath solution is provided next to the current trace. *B*, reversal potentials obtained with outside-out patches. The concentration of the KCl in the bath solution is provided next to the current trace. In all cases, the pipette solution contained 100 mM KCl. Current traces were obtained with the application of ±70 mV voltage ramps and digitally filtered at 500 Hz for presentation.

the extracellular surface is exposed to low ionic strength solutions and decreases when it is exposed to high ionic strength solutions (Fig. 2*A*, Table 2). Changing the ionic strength at the intracellular surface of the unapposed hemichannel has less effect on the reversal potential and consequently the charge selectivity of the hemichannel than comparable changes at the extracellular surface (Fig. 2*A*). Taken together, the results suggest that negative charge(s) on the extracellular surface of the Cx32*43E1 hemichannel play a substantial role in establishing the cation selectivity. The inward rectification of the current–voltage relation of the open Cx32*43E1 hemichannel in symmetric salt conditions can also be explained by the presence of a negative charge located near the extracellular end of the channel pore.

A role for negative charges in the first extracellular loop (E1) in determining the charge selectivity of unapposed connexin hemichannels is expected based on the studies of Cx46 charge selectivity by Trexler *et al.* (2000). The properties of the Cx46 channel could be replicated with a permeation model developed by Chen & Eisenberg (1993) that solves the Poisson–Nernst–Plank (PNP) equations in one dimension (Trexler *et al.* 2000). The Cx46 model channel contained a single negative charge region centred at a distance 0.75 (from the cytoplasmic end of the channel) at a concentration of $4\,\mathrm{mol\,l^{-1}}$. This simple charge distribution correctly predicted the reversal potentials and the current–voltage relation of the Cx46 channel in a variety of recording configurations that altered the ionic strength of the bath solutions. Trexler *et al.* (2000) concluded that negative charges in E1 are the major determinants of the charge selectivity of Cx46 channels and proposed that charged residues in E1 act as a charge selectivity filter.

Figure 6*A* illustrates a modification of the Cx46 charge distribution model for the Cx32*43E1 hemichannel. In this model, the magnitude of the negative charge region is reduced to $1\,\mathrm{mol\,l^{-1}}$ to reflect the reduced cation selectivity of the Cx32*43E1 hemichannel and the charged region was centred at a position of 0.8 to better match the degree of rectification observed for the 43E1 hemichannel in symmetric salt (not shown). The channel length was increased from 50 to 60 Å and the pore radius increased to 7 Å in accordance with experimental measurement (Oh *et al.* 1997). Reversal potentials and P_K/P_{Cl} ratios are presented in tabular form and the absolute values of the reversal potentials are plotted as a function of salt concentration in Fig. 6*A* to allow comparison with the Cx32*43E1 data set (Fig. 2*A*).

The permeability of the model channel qualitatively replicates many of the properties of the Cx32*43E1 hemichannel. The cation selectivity of the model channel is maximal when the extracellular surface (outside-out patch) is exposed to 10 mM KCl ($E_{rev} = -42.2$; $P_K/P_{Cl} = 12.8$) and decreases as the salt concentration is increased to 500 mM KCl ($E_{rev} = 7.3$; $P_K/P_{Cl} = 1.6$). The data obtained for Cx32*43E1 follow the same relation, the reversal potentials are maximal in outside-out patches in 10 mM KCl and decrease as the concentration of external salt is increased (Fig. 2*A*, Table 2). The change in charge selectivity is a consequence of changes in the degree of charge screening that is expected to occur as the salt concentration is altered. The cation selectivity of the channel is expected to decrease when a negative charge located near the extracellular entrance of the channel is progressively screened by the addition of more salt to the extracellular bath. The result is not surprising as PNP is essentially a theory of screening fixed charges by mobile charge (Chen & Eisenberg 1993).

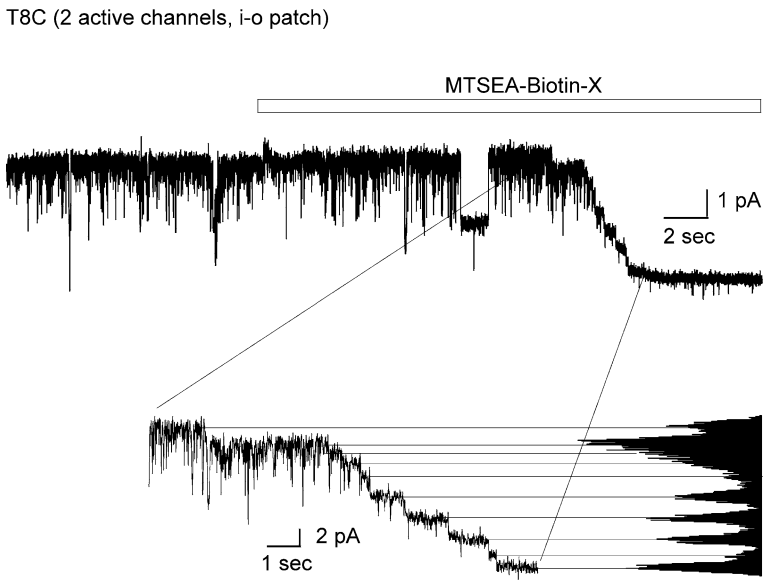

Figure 5. The modification of an inside-out patch containing two active T8C channels by MTSEA biotin-X
Current was elicited at a holding potential of −60 mV. The duration of time at which 1 mM MTSEA biotin-X was perfused is indicated by the shaded bar. Expanded section of the record illustrates nine stepwise changes in conductance indicating modification of at least 9 of 12 T8C residues with MTSEA biotin-X.

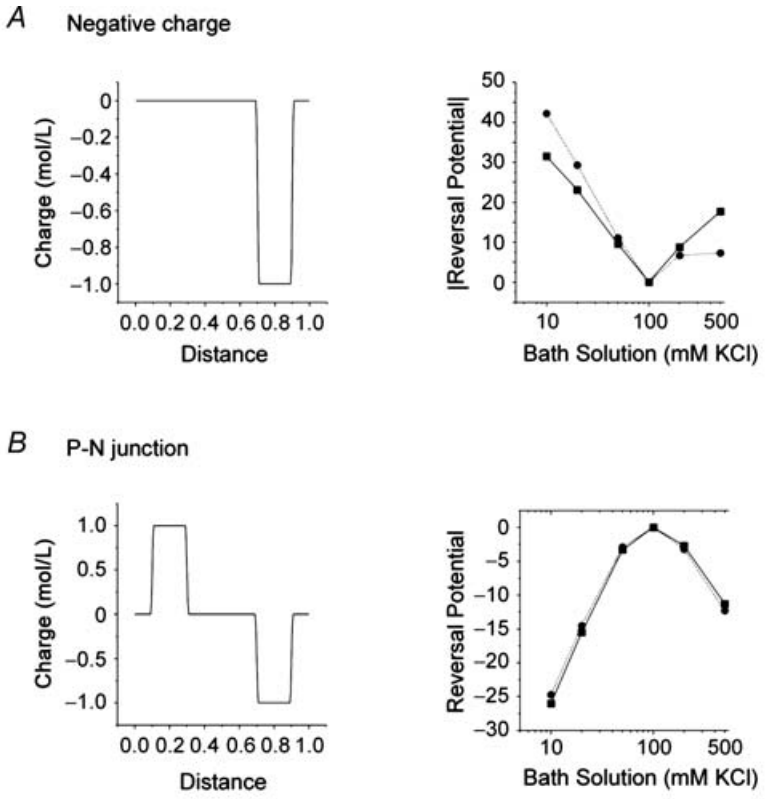

A Negative charge		Bath Solution				
		10 mM	20 mM	50 mM	200 mM	500 mM
O/O patch	E_{rev}	-42.2	-29.3	-11.1	6.7	7.3
	P_K/P_{Cl}	12.8	9.4	5.6	2.5	1.6
I/O patch	E_{rev}	31.5	23.1	9.6	-8.8	-17.7
	P_K/P_{Cl}	5.5	4.9	4.1	3.5	3.3
B P-N junction						
O/O patch	E_{rev}	-24.7	-14.5	-2.9	-3.2	-12.3
	P_K/P_{Cl}	3.6	2.5	1.5	0.66	0.45
I/O patch	E_{rev}	-26	-15.5	-3.4	-2.7	-11.3
	P_K/P_{Cl}	0.26	0.37	0.64	1.4	2.1

Figure 6. Reversal potentials of model channels determined with numerical solution of PNP equations provided by Chen & Eisenberg (1993)
A, left panel, the charge distribution model of a channel containing a single region of negative charge (3*e* positioned at a distance from 0.75 to 0.85). This corresponds to a charge density of 1 mol l^{-1} for a channel modelled as a right cylinder 60 Å long, 7 Å radius. Right panel, the absolute values of reversal potentials for inside-out and outside-out conditions are plotted as a logarithmic function of salt concentration. ■ denotes inside-out patch configuration; ● denotes outside-out patch configuration. The reversal potentials calculated for outside-out (O/O) and inside-out (I/O) are presented in part A of the Table for ionic conditions comparable to those used in this study. In all cases the opposing solution contained 100 mM KCl. Ionic activities used in the calculation of P_K/P_{Cl} ratios are those listed in Table 2 for a given salt concentration. *B*, left panel, a charge distribution model of a P–N junction containing a region of positive charge located near the intracellular end of the pore and a region of negative charge located near the extracellular end of the pore. Right panel, absolute values of reversal potentials of the P–N junction are plotted against the logarithm of salt concentration. ■ denotes inside-out patch configuration; ● denotes outside-out patch configuration. The reversal potentials and P_K/P_{Cl} ratios determined for the model channel shown in the left panel of *B* with the PNP equations are presented in part B of the table.

The cation selectivity of the model channel is reduced when the salt concentration of the internal solution is varied to correspond to an inside-out patch configuration. Cation selectivity is maximal when the internal surface of the channel is bathed in low salt ($E_{rev} = 31.5$; $P_K/P_{Cl} = 5.5$ in 10 mM KCl) and decreases as the salt concentration in the bath is increased ($E_{rev} = -17.7$; $P_K/P_{Cl} = 3.3$ in 500 mM KCl). As expected, charges located at the extracellular end of the channel are less sensitive to screening by salt applied from the intracellular side of the channel and consequently the charge selectivity of the channel is maximal when the extracellular surface of the channel is exposed to low ionic strength solutions.

Although the model channel qualitatively describes the charge selectivity of the Cx32*43E1 hemichannel, there is a large discrepancy in the magnitude of reversal potentials in inside-out and outside-out patches (compare Fig. 2*A* with Fig. 6*A*) and the cation selectivity of the model channel is much greater than what is observed in spite of the low charge density used in the charge distribution model. A second major discrepancy is the current–voltage relation of the model and Cx32*43E1 hemichannel in outside-out patches in 500 mM KCl. The current–voltage relation of the Cx32*43E1 hemichannel rectifies outwardly in this condition and inwardly in all other conditions (Fig. 1). In contrast, the *I–V* relation of the model channel rectifies inwardly for all charge distributions that contain a single region of negative charge located in the pore towards the extracellular end of the channel (not shown). The discrepancies suggest, at least within the limitations of the one dimensional PNP model employed, that additional charges may be present, which determine the charge selectivity and shape the *I–V* relations of Cx32*43E1 hemichannels. In addition, the PNP model employed utilizes a pore of constant geometry and there is no reason to believe that the hemichannel conforms to this assumption (see below). Consequently, we did not attempt to exhaustively explore charge distribution models that incorporated additional regions of charge.

Our previous studies have implicated a role of a positive charge located in the N-terminus of Cx32 and Cx32*43E1 in determining the polarity of voltage dependence (Verselis *et al.* 1994; Oh *et al.* 2000), the electrical rectification of single channel conductance of heterotypic Cx32 and Cx26 junctions (Oh *et al.* 1999), and the slight anion selectivity of human Cx32 junctions (Oh *et al.* 1997). However, a positive charge located in this position coupled with a negative charge at the extracellular end of an unopposed hemichannel would result in the formation of a P–N junction, whose properties differ substantially from those observed in this study.

The properties of a P–N junction, formed by the placement of a negative charge at the extracellular end of the channel and a positive charge at the intracellular end of the channel, are presented in Fig. 6*B*. The model channel exhibits a preference for cations when the internal positive charge is screened by exposure to high concentrations of KCl and switches to become anion selective when this charge is exposed to low concentrations of KCl. A similar pattern is observed when the external salt concentration is varied: the channel is cation selective when the negative charge at the extracellular end of the channel pore is exposed to low salt, and becomes anion selective when this charge is screened by high salt concentrations. The change in charge selectivity is a consequence of differential screening of charges at opposite ends of the channel. The small difference in reversal potentials for inside-out and outside-out patches that is predicted by the PNP model is a consequence of the different mobility of potassium and chloride ions used in the solution of the PNP equations. Kienker *et al.* (1994), Kienker & Lear (1995), and Chen *et al.* (1997) reported qualitatively similar behaviour for the synthetic LS channel. Thus, the incorporation of a positive charge into the N-terminus of Cx32*43E1 hemichannel cannot account by itself for the observed deviation in channel properties from that predicted by a simple model channel containing a region of negative charge at the extracellular end.

Yet, the data presented here strongly support the view that charges in the N-terminus can play an important role in determining the charge selectivity of Cx32*43E1 channels as the addition of negative charge at either the 2nd, 5th or 8th position increases both the cation selectivity and the unitary conductance of the Cx32*43E1 channel and linearizes the open channel *I–V* relation, while the substitution of positive charge at the 5th position decreases cation selectivity and unitary conductance (Fig. 2*E* and *F* and Table 2) and slightly increases the amount of inward rectification (Fig. 4).

The principle feature of the N2E and G5D data sets is the marked increase in reversal potentials and cation selectivity relative to Cx32*43E1 in inside-out patches under all ionic conditions (Fig. 2). Exposure of the intracellular face of the channel to low salt is expected to maximize the contribution of charges in the N-terminus in determining charge selectivity as a consequence of reduced charge screening. Screening of N-terminal charges by exposure of the intracellular surface to high ionic strength bath solutions should unmask the contribution of negative charge located near the extracellular face of the channel in determining charge selectivity. Thus, the addition of negative charge to the intracellular end is expected to increase cation selectivity in all salt gradients that vary the ionic strength of the bath solution. This is what is observed (Fig. 2).

In outside-out patches the reversal potentials of N2E and G5D channels are similar or slightly larger than those of Cx32*43E1 in salt gradients that expose the extracellular surface of the channel to low ionic strength bath solutions (Fig. 2*D*). With these conditions, extracellular

charges are expected to make a substantial contribution to determining charge selectivity. The linearity of the current–voltage relation observed when the extracellular surface of the N2E channel is exposed to 10 mM salt (Fig. 3*C*) can be ascribed to the influence of a negative charge at the extracellular end of the channel. Note that the current–voltage relation of Cx32*43E1 rectifies inwardly in this condition (Fig. 1*B*). When extracellular charges are exposed to high ionic strength solutions, charges located at the internal end (N-terminus) are expected to cause an increase in the measured reversal potential relative to the Cx32*43E1 channel. This is what is observed: the reversal potentials of N2E and G5D in outside-out patches are much larger than those observed for Cx32*43E1 (Fig. 2*D* and *F*).

The similarity in the reversal potential–bath ionic strength relation for inside-out and outside-out patch configurations of N2E (Fig. 2*B*) suggests that negative charges at the intracellular end and extracellular end of the channel may make approximately equal contributions in determining charge selectivity. The reversal potentials of inside-out and outside-out patches are predicted to have the same absolute values with a charge distribution model that places fixed charges of the same sign symmetrically at opposite ends of the channel (not shown). However, the slight outward rectification of the open N2E current–voltage relation (Fig. 3*A*) and linearity of G5D in symmetric salt suggests that intracellular (N-terminal) charges at the 2nd position may have a larger effect in determining charge selectivity than those located in the extracellular region in these conditions. Similarly, the larger reversal potential obtained for N2E outside-out patches exposed to 500 mM salt relative to inside-out patches with the same conditions (32.3 ± 2.4 mV *versus* 23.8 ± 1.7 mV, respectively, Fig. 2*B*) is predicted by the PNP model if the magnitude of negative charge at the intracellular end of the channel is greater than that assigned to the extracellular end of the channel (see Fig. 7). There is little difference in the absolute values of the reversal potentials for these conditions with G5D (28.5 ± 4.9 mV *versus* 26.6 ± 2.4 mV, outside-out *versus* inside-out in 500 mM KCl, respectively). This again supports the view that a negative charge at the 5th position has a smaller effect in determining the cation selectivity than a negative charge at the 2nd position.

While the reversal potentials and conductance of N2E and G5D channels are similar, the reversal potentials and conductance of T8D channels are less than those of N2E and G5D channels but greater than Cx32*43E1 in inside-out patches (Fig. 2*C* and *D*). In outside-out patches, the measured reversal potentials are similar for N2E, T8D and Cx32*43E1 in low salt, a condition that is expected to increase the influence of extracellular charges. In high salt, a condition that is expected to expose the influence of intracellular charges, the measured reversal potentials of T8D are larger than Cx32*43E1 but less than N2E (Fig. 2*D*). Taken together, these results indicate that a negative charge at the 8th position has less influence on charge selectivity than do negative charges at the 2nd or 5th positions.

The reduction in conductance and charge selectivity that occurs when a negative charge is moved from the 2nd or 5th to the 8th position cannot be explained by simply repositioning the negative charge closer to the

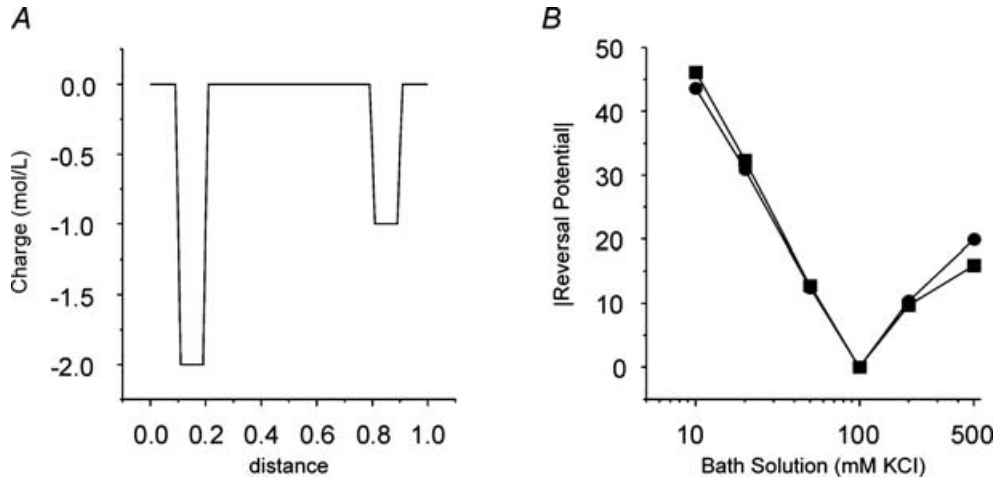

Figure 7. Reversal potentials of model channels determined with numerical solution of PNP equations provided by Chen & Eisenberg (1997)
A, a charge distribution model of a channel containing two regions of negative charge; the internal charge of 2 M/L is positioned at distance 0.1–0.2, the external charge 1 mol l^{-1} is positioned at distance 0.8–0.9. *B*, the absolute values of reversal potentials for inside-out and outside-out conditions are plotted as a logarithmic function of salt concentration. ■ denotes inside-out patch configuration; ● denotes outside-out patch configuration.

intracellular surface of a right cylindrical channel that is used in the PNP model. If the N-terminus has helical character as indicated by structural studies (Purnick *et al.* 2000*a*), then the distance between the C-α carbons of the 2nd and 8th and 5th and 8th residues is approximately 10 and 5 Å, respectively. If we assume that the channel is 60 Å, then a charge at the 8th position would be ~0.16 distance units closer to the intracellular end of the channel than a charge at the 2nd position. The inward movement (toward the cytoplasmic end) of the negative charge to this position results in small changes in the charge selectivity and conductance of a channel modelled with PNP (not shown). A possible explanation for the reduced cation selectivity and conductance of T8D is that the diameter of the channel is larger in the vicinity of the 8th residue than at the 2nd or 5th residues. An increase in pore diameter in the vicinity of the 8th residue would reduce the effective concentration of fixed negative charge on the pore surface leading to a reduction in the local concentration of mobile counter-ions. Consequently, both conductance and cation selectivity would be expected to decrease. This explanation is supported by the demonstration that the T8C residue resides in the intracellular region of the pore (Fig. 5) and by the structure of the N-terminus provided by Purnick *et al.* (2000*a*), which indicates that residues at the 2nd and 5th position are also pore lining given that the 8th residue is positioned within the pore. The structure provided by Purnick *et al.* (2000*a*) also indicates that the N-terminus flares outwardly.

In contrast to a negative charge substitution at the 5th position, the substitution of a positive charge, G5R, substantially reduces cation selectivity and unitary conductance. The reversal potentials of G5R hemichannels are close to 0 mV in all conditions examined, indicating that the channel is essentially non-selective (Table 2, Fig. 2*E* and *F*). Notably, G5R reduces the unitary conductance of G5D from 240 to 70 pS in 100 mM symmetric salt. As with the 43E1 hemichannel, the charge selectivity of G5R cannot be explained by simply positioning a positive charge in the N-terminus in the absence of some additional intracellular negative or extracellular positive charge because this would result in the formation of a P–N junction. The decrease in unitary conductance together with the reduction in cation selectivity suggests that a positive charge at the 5th position acts as a barrier reducing cation flux rather than simply increasing the local concentration of anions and consequently increasing the contribution of anion flux to total current. This possibility suggests that there may be additional negative charges lying closer to the intracellular end of the channel or on the channel surface that may bias the channel toward cation selectivity. Banach *et al.* (2000) have reported that fixed negative surface charges positioned adjacent to the intracellular entrance of channel pore adequately model the conductance of human Cx37 intercellular channels. Negative surface charges would be expected to increase the local concentration of cations and decrease the concentration of anions at the entry of the channel. The addition of negative charge at the 2nd, 5th and 8th positions in the N-terminus would further increase the local concentration of cations and consequently increase the cation selectivity and conductance of these channels. The presence or addition of positive charges at the 5th (G5R), 2nd (N2R/K) or 1st (wild-type) positions could form an electrostatic 'barrier' that would reduce cation flux and also preclude the formation of a P–N junction. The reduction in unitary conductance that results from such an electrostatic effect could occur independently of pore diameter and could explain the low conductance in spite of the large pore diameter of the Cx30.2 channels as reported by Bukauskas *et al.* (2006) and Rackauskas *et al.* (2007).

Although the unitary conductance of the N2E + G5R hemichannel is similar to that of the parental Cx32*43E1 hemichannel, the reversal potentials in inside-out patches lie between those obtained for negative charge substitutions at either the 2nd or 5th position and the Cx32*43E1 hemichannel (Fig. 2*E*). This also supports the view that a negative charge at the 2nd residue has a larger effect in determining the charge selectivity of the channel than do charges located at the 5th position. If this were not the case, one would expect that charges of equal but opposite valence at the 5th and 2nd positions would effectively cancel resulting in charge selectivity identical to Cx32*43E1. A similar conclusion is reached if one considers unitary conductance. Oh *et al.* (2004) report the unitary conductance of N2R + G5D to be less than that of N2E + G5R and N2E + G5K, 105 *versus* 120 pS, respectively. Thus, the sign of the charge at the 2nd position appears to play a larger role in determining unitary conductance than at the 5th residue. However, the sign of the charge at the 5th position has a larger role in shaping the open channel current–voltage relation in symmetric salt than the 2nd residue. The current–voltage relations of N2E + G5K and N2E + G5R hemichannels rectify inwardly in symmetric salt while that of N2R + G5D is linear (Oh *et al.* 2004). This result can be replicated with the PNP model using a modification of the charge distribution model shown in Fig. 7 that incorporates regions of positive and negative charge at the intracellular end if the magnitude of the charge lying deeper in the pore is slightly greater than the more intracellularly located charge (not shown), but again such models do not correctly predict the reversal potentials or *I–V* relations under all conditions (not shown).

The inability of simple charge distribution models, which place charges at either end of the hemichannel, to fit the experimental data suggests that other charged residues play a role in determining the charge selectivity of wild-type and mutant Cx32*43E1 hemichannels if we

assume a uniform channel diameter. The most obvious candidates are highly conserved charged residues located within transmembrane segments which may line or lie in close proximity to the channel pore (see Zhou *et al.* 1997; Skerrett *et al.* 2002). These include the positively charged residue R32 located in the centre of TM1 and a positive and negative charge in TM3. The positive residue, R142, is centrally located in TM3, while the negative residue, E146, is likely to lie closer to the extracellular end of the channel. However, in the absence of surface charge, the placement of charges in these positions would essentially maintain the P–N junction illustrated in Fig. 6*B*, i.e. the positive charges are segregated toward the internal surface of the channel, the negative charges segregated toward the external surface of the channel.

The emerging view is that molecular determinants of charge selectivity, conductance and the *I–V* relations of the Cx32*43E1 hemichannel are likely to involve charged residues located at the extracellular end of the channel. However, the placement of charges at other locations, notably at the intracellular end or over the surface of the channel, can have a substantial if not larger effect on the charge selectivity of the Cx32*43E1 hemichannel. Support for a major role of E1 in determining charge selectivity of Cx46 has been provided by Kronengold *et al.* (2003). This study reported that the substitution of the E1 domain of Cx32 or Cx43 into Cx46 (Cx46*32E1 and Cx46*43E1) changed the charge selectivity of the Cx46 hemichannel from cationic to anionic in the case of Cx46*32E1 and to non-selective in the case of Cx46*43E1, although the latter was assessed solely by the transfer of both cationic and anionic dyes. The direction of open channel current rectification of the Cx46 hemichannel was also changed from inward to outward for Cx46*32E1 consistent with the presence of an extracellular positive charge.

The difference in the properties of the Cx46*32E1 chimera was attributed to a difference in the charge of two residues in E1 of Cx32 and Cx46, Cx32K48 and Cx32S50 (see Table 1, but note the difference in numbering). These residues are Q49 and D51 in the actual sequence of Cx43 and Cx46, thus the Cx46*32E1 chimera contains a positive charge at the 48th position and a neutral charge at the 50th position (Table 1). Mutation of these residues in the Cx46*32E1 chimera to those present in Cx46, i.e. K48(49)Q and S50(51)D, resulted in a cation selective, inward rectifying channel similar to wild-type Cx46. The Cx46*32E1 chimera would also lose the negatively charged Cx46E61 residue and substitute R67H. The role of these latter two residues in determining the charge selectivity of the Cx46*32E1 chimera was not determined.

A puzzling feature of these results is how the substitution of Cx43E1 into Cx46 produces a non-selective channel while the same substitution in Cx32 results in a cation selective channel. The divergence of the sequence of E1 in the three connexins most likely contributes to the difference in charge selectivity (Table 1). The sequence of Cx46 is characterized by a high density of negative charge lying toward the M1–E1 border. Of the negatively charged residues in Cx46, two, E43 (E42, Table 1) and D51 (D50, Table 1), line the channel pore (Kronengold *et al.* 2003). Modification of Cx46D51C with the positively charged MTSET reagent substantially reduces single channel conductance, changes the *I–V* relation from strong inward to slight outward rectification, and decreases the cation selectivity of the channel (V. K. Verselis, unpublished observation) while modification of Cx46D51C with the negatively charged MTSES reagent converts D51C channels to wild-type (Kronengold *et al.* 2003). We propose that the presence of negative charges at E43 and D51 underlies the dominance of E1 in determining the charge selectivity of the wild-type Cx46 channel because these residues line the aqueous pore. Substitution of either Cx32E1 or Cx43E1 into Cx46 removes both negative charges. We assert that the resulting charged residues in the Cx46 chimeras, which are located in different positions, are less effective in determining charge selectivity than E43 and D51, perhaps because they are not pore lining or because the extracellular end of the Cx46 channel flares outwardly from residue D51. Consequently, the contributions of charged residues located in other regions of the channel are unmasked in these chimeras and these residues differ in Cx32 and Cx43. This could explain how the substitution of the Cx43E1 into Cx46 produces a non-selective channel while the same substitution in Cx32 results in a cation selective channel and also explain the potential dominance of negative charges in the N-terminus in determining ion flux through the Cx32*43E1 chimera.

This study reveals several principles that are likely to underlie the complex relation between the perm-selectivity and conductance reported in studies of naturally occurring connexin channels. The results presented in this paper lead to the view that charge selectivity and conductance are determined in part by the combined effects of charged residues that can be dispersed within the channel pore and over the surface of the channel. The contribution of a given charged residue to charge selectivity would depend upon its relative location in the channel pore, the diameter of the pore in the vicinity of the charged residue and the relative position of the given charge to other charged residues. In channels that contain negative charges at both ends, such as N2E, approximately 90% of current is predicted by PNP models to be carried by cations under physiological conditions. The presence of a negative surface charge would also tend to bias connexin channels toward cation selectivity. Screening of negatively charged residues by divalent cations could provide a physiological mechanism to modulate the perm-selectivity of signalling molecules that are expected to function in development and physiological processes.

The strong correlation between unitary conductance and charge selectivity indicates that the permeability of Cx32*43E1 and Cx46 channels to small metallic ions is largely electrostatic. This view differs from that advanced by Skerrett *et al.* (2002) in which, the selective permeability of Cx32 gap junctions were proposed to result 'from novel mechanisms including complex van der Waals interactions of permeants with the pore wall, rather than mechanisms involving fixed charges or chelation chemistry as reported for other ion channels'.

References

Banach K, Ramanan SV & Brink PR (2000). The influence of surface charges on the conductance of the human connexin37 gap junction channel. *Biophys J* **78**, 752–760.

Beblo DA & Veenstra RD (1997). Monovalent cation permeation through the connexin40 gap junction channel: Cs, Rb, K, Na, Li, TEA, TMA, TBA, and effects of anions Br, Cl, F, acetate, aspartate, glutamate, and NO_3. *J Gen Physiol* **109**, 509–522.

Bennett MV, Zheng X & Sogin ML (1994). The connexins and their family tree. *Soc Gen Physiol Series* **49**, 223–233.

Brink PR (1983). Effect of deuterium oxide on junctional membrane channel permeability. *J Membr Biol* **71**, 79–87.

Bukauskas FF, Bukauskiene A & Verselis VK (2002). Conductance and permeability of the residual state of connexin43 gap junction channels. *J Gen Physiol* **119**, 171–186.

Bukauskas FF, Kreuzberg MM, Rackauskas M, Bukauskiene A, Bennett MV, Verselis VK & Willecke K (2006). Properties of mouse connexin 30.2 and human connexin 31.9 hemichannels: implications for atrioventricular conduction in the heart. *Proc Natl Acad Sci U S A* **103**, 9726–9731.

Chen D & Eisenberg R (1993). Charges, currents and potentials in ionic channels of one conformation. *Biophys J* **64**, 1405–1421.

Chen D, Lear J & Eisenberg B (1997). Permeation through an open channel: Poisson-Nernst-Planck theory of a synthetic ionic channel. *Biophys J* **72**, 97–116.

Dong L, Liu X, Li H, Vertel BM & Ebihara L (2006). Role of the N-terminus in permeability of chicken connexin45.6 gap junctional channels. *J Physiol* **576**, 787–799.

Eisenman G & Horn R (1983). Ionic selectivity revisited: the role of kinetic and equilibrium processes in ion permeation through channels. *J Membr Biol* **76**, 197–225.

Gil Z, Magleby KL & Silberberg SD (1999). Membrane–pipette interactions underlie delayed voltage activation of mechanosensitive channels in *Xenopus* oocytes. *Biophys J* **76**, 3118–3127.

Harris AL (2001). Emerging issues of connexin channels: Biophysics fills the gap. *Q Rev Biophys* **34**, 325–472.

Harris AL (2007). Connexin channel permeability to cytoplasmic molecules. *Prog Biophys Mol Biol* **94**, 120–143.

Hu X, Ma M & Dahl G (2006). Conductance of connexin hemichannels segregates with the first transmembrane segment. *Biophys J* **90**, 140–150.

Kienker PK, DeGrado WF & Lear JD (1994). A helical-dipole model describes the single-channel current rectification of an uncharged peptide ion channel. *Proc Natl Acad Sci U S A* **91**, 4859–4863.

Kienker PK & Lear JD (1995). Charge selectivity of the designed uncharged peptide ion channel Ac-(LSSLLSL) 3-CONH2. *Biophys J* **68**, 1347–1358.

Kronengold J, Trexler EB, Bukauskas FF, Bargiello TA & Verselis VK (2003). Single-channel scam identifies pore-lining residues in the first extracellular loop and first transmembrane domains of cx46 hemichannels. *J Gen Physiol* **122**, 389–405.

Ma M & Dahl G (2006). Cosegregation of permeability and single-channel conductance in chimeric connexins. *Biophys J* **90**, 151–163.

Oh S, Abrams CK, Verselis VK & Bargiello TA (2000). Stoichiometry of transjunctional voltage-gating polarity reversal by a negative charge substitution in the amino terminus of a connexin32 chimera. *J Gen Physiol* **116**, 13–31.

Oh S, Ri Y, Bennett MV, Trexler EB, Verselis VK & Bargiello TA (1997). Changes in permeability caused by connexin 32 mutations underlie X-linked Charcot-Marie-Tooth disease. *Neuron* **19**, 927–938.

Oh S, Rivkin S, Tang Q, Verselis VK & Bargiello TA (2004). Determinants of gating polarity of a connexin 32 hemichannel. *Biophys J* **87**, 912–928.

Oh S, Rubin JB, Bennett MV, Verselis VK & Bargiello TA (1999). Molecular determinants of electrical rectification of single channel conductance in gap junctions formed by connexins 26 and 32. *J Gen Physiol* **114**, 339–364.

Purnick PE, Benjamin DC, Verselis VK, Bargiello TA & Dowd TL (2000*b*). Structure of the amino terminus of a gap junction protein. *Arch Biochem Biophys* **381**, 181–190.

Purnick PE, Oh S, Abrams CK, Verselis VK & Bargiello TA (2000*a*). Reversal of the gating polarity of gap junctions by negative charge substitutions in the N-terminus of connexin 32. *Biophys J* **79**, 2403–2415.

Qu Y & Dahl G (2002). Function of the voltage gate of gap junction channels: selective exclusion of molecules. *Proc Natl Acad Sci U S A* **99**, 697–702.

Rackauskas M, Verselis VK & Bukauskas FF (2007). Permeability of homotypic and heterotypic gap junction channels formed of cardiac connexins mCx30.2, Cx40, Cx43, and Cx45. *Am J Physiol Heart Circ Physiol* **293**, H1729–H1736.

Skerrett IM, Aronowitz J, Shin JH, Cymes GE, Kasperek E, Cao FL & Nicholson BJ (2002). Identification of amino acid residues lining the pore of a gap junction channel. *J Cell Biol* **159**, 349–360.

Srinivas M, Calderon DP, Kronengold J & Verselis VK (2006). Regulation of connexin hemichannels by monovalent cations. *J Gen Physiol* **127**, 67–75.

Trexler EB, Bukauskas FF, Kronengold J, Bargiello TA & Verselis VK (2000). The first extracellular loop is a major determinant of charge selectivity in connexin46 channels. *Biophys J* **79**, 3036–3051.

Verselis VK & Brink PR (1986). The gap junction channel: its aqueous nature as indicated by deuterium oxide effects. *Biophys J* **50**, 1003–1007.

Verselis VK, Ginter CS & Bargiello TA (1994). Opposite voltage gating polarities of two closely related connexins. *Nature* **368**, 348–351.

Wang HZ & Veenstra RD (1997). Monovalent ion selectivity sequences of the rat connexin43 gap junction channel. *J Gen Physiol* **109**, 491–507.

Zhou XW, Pfahnl A, Werner R, Hudder A, Llanes A, Luebke A & Dahl G (1997). Identification of a pore lining segment in gap junction hemichannels. *Biophys J* **72**, 1946–1953.

Acknowledgements

We thank Angele Bukauskiene and Joe Zavilowitz for technical assistance and Duan Chen and Brady Trexler for providing computer programs for the solution of PNP equations. The paper is dedicated to the memory of Joe Zavilowitz. This work was supported by the National Institutes of Health grant GM 46889.

Author's present address

S. Oh: Department of Physiology, College of Medicine, Dankook University, Cheonan City, Korea 330-714.